

Clauser–Horne inequality for the full counting statistics

This article has been downloaded from IOPscience. Please scroll down to see the full text article.

2005 New J. Phys. 7 183

(<http://iopscience.iop.org/1367-2630/7/1/183>)

View [the table of contents for this issue](#), or go to the [journal homepage](#) for more

Download details:

IP Address: 38.107.179.212

The article was downloaded on 20/02/2012 at 10:18

Please note that [terms and conditions apply](#).

Clauser–Horne inequality for the full counting statistics

Fabio Taddei¹, Lara Faoro², Elsa Prada^{3,4} and Rosario Fazio¹

¹ NEST-INFM & Scuola Normale Superiore, I-56126 Pisa, Italy

² Department of Physics and Astronomy, Rutgers University, 136 Frelinghuysen Road, Piscataway, NJ 08854, USA

³ Departamento de Física Teórica de la Materia Condensada, C-V, Universidad Autónoma de Madrid, E-28049 Madrid, Spain

⁴ Institut für Theoretische Festkörperphysik, Universität Karlsruhe, D-76128 Karlsruhe, Germany

E-mail: f.taddei@sns.it

New Journal of Physics **7** (2005) 183

Received 7 June 2005

Published 26 August 2005

Online at <http://www.njp.org/>

doi:10.1088/1367-2630/7/1/183

Abstract. We discuss the Clauser–Horne (CH) inequality for electrons in mesoscopic systems formulated in terms of the full counting statistics (FCS). A derivation of such an inequality is provided for a prototype setup consisting of an entangler attached to two conducting wires, that brings pairs of spin-entangled electrons into spatially separated counters, where detection takes place. Violation of the CH inequality is analysed as a function of the various parameters characterizing the system. The effect of dephasing, which can occur in realistic wires, is also addressed. As expected, the extent of violation is monotonically suppressed by increasing dephasing strength. The CH inequality is finally applied to a three-arm normal-metallic beam splitter. Our results show that violation takes place even in the absence of interaction.

Contents

1. Introduction	2
2. The prototype setup	3
3. Derivation of the CH inequality	4
4. Scattering approach to the full-counting statistics	5
5. Entangled electrons	7
6. Effect of dephasing	12
7. Normal beam-splitter	16
8. Conclusions	19
Acknowledgments	19
References	19

1. Introduction

Quantum information is a young and very attractive field of research both from a fundamental point of view and because of its important potential applications. Entanglement [1] is the most important resource for the implementation of quantum computation and quantum communication schemes [2]. Most of the work on entanglement has been carried out in optical systems with photons [3], cavity QED systems [4] and ion traps [5]. Only recently has attention been devoted to the manipulation of entangled electronic states in a solid-state environment [6]–[8]. This is a very attractive area of research that can profit from the vast technological knowledge available and which allows, in the perspective of future applications, for scalability and integration. A number of different realizations of entangled electrons have since been proposed: hybrid normal-superconducting structures [9]–[15], superconductor–carbon nanotube systems [16]–[18] quantum dots in the Coulomb blockade regime [6, 19, 20], chaotic quantum dots [21], Kondo-like impurities [22], quantum Hall bar systems [23], [27]–[30], Coulomb scattering in 2D electron gas [31].

By coupling the source of entanglement to a beam-splitter, entanglement can be detected in the transported quantities, such as current fluctuations [32] and full counting statistics (FCS) [33]. Furthermore, the entanglement can be detected by means of a Bell inequality [34] and quantities like concurrence [35], expressed in terms of zero-frequency current noise [10, 11], [23]–[26], [29, 36]. Violation of a Bell inequality implies that there exist quantum correlations between the detected particles that cannot be described by any local hidden variables theory.

In the present paper, we review our work on the Clauser–Horne (CH) inequality [41, 42] for the FCS and provide some additional results with respect to [37, 47]. We shall show that the joint probabilities for a given number of electrons to pass through a mesoscopic conductor (in a given time) should satisfy, for a classical local theory, an inequality. We consider as a prototype setup a generic entangler connected to two conducting wires, which carry the entangled electrons into two spatially separated regions. Detection is performed by spin-selective counters along a given local spin quantization axis. In the case where only two entangled electrons are injected, we find a situation similar to that with photons. More generally, we discuss the case where a large number of electrons are injected, finding that the CH inequality is violated virtually only when a ‘coincidence measurement’ is performed.

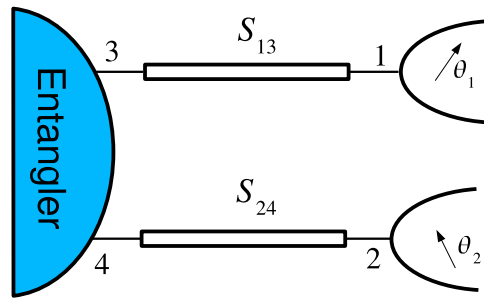


Figure 1. Idealized setup for testing the CH inequality for electrons in a solid-state environment. It consists of two parts: an entangler (shaded block) that produces pairs of spin entangled electrons exiting from terminals 3 and 4. These terminals are connected to leads 1 and 2 through two conductors described by scattering matrices S_{13} and S_{24} . Electron counting is performed in leads 1 and 2 along the local spin-quantization axis oriented at angles θ_1 and θ_2 .

While traversing the conductors, before reaching the detectors, electrons might be subjected to decoherence. In this work, the effect of decoherence is mimicked by including additional fictitious leads along both wires [48]. In the rest of the paper, we shall refer to the effect produced by such additional leads as decoherence, in a loose sense.

The paper is organized as follows: in section 2, we describe in detail the mesoscopic system we are considering to test the violation of the CH. In section 3, we present the derivation of the CH inequality for the FCS and in section 4 we resume, for completeness, the relation between FCS and the scattering matrix. The results for an idealized entangler are presented in section 5, where a systematic analysis of the violation of the CH inequality against all the parameters of the device is presented. Section 6 is devoted to the study of the effect of decoherence on the violation of the CH inequality, while in section 7, we consider a realistic system, namely a three-arm normal beam-splitter. Concluding remarks are given in section 8.

2. The prototype setup

FCS refers to the probability that a given number of electrons have traversed a mesoscopic conductor in a time t . In the long-time limit, the first and second moment of the probability distribution are related to the average current and noise, respectively. In its original version [34], the Bell inequality was derived for dichotomic variables. Here, we resort to the more general formulation due to Clauser and Horne [41]. To this aim, we consider the idealized setup, illustrated in figure 1, which consists of the following parts. On the left, we place an entangler that produces pairs of electrons in a spin-entangled state. Each electron propagates respectively into lead 3 and 4 in a superposition of spin states \uparrow and \downarrow . Two conductors, characterized by some scattering matrix, connect the terminals 3 and 4 of the entangler with the exit leads 1 and 2, so as to carry the two particles belonging to each pair into two different spatially separated reservoirs. The electron counting is performed in leads 1 and 2 for electrons with spin aligned along the local spin-quantization axis at angles θ_1 and θ_2 . Detection is realized by means of spin-selective counters, i.e. by counting electrons with the projection of the spin along a given

local quantization-axis. In analogy with the optical case, we say that the analyser is not present, when the electron counting is spin-insensitive (electrons are counted irrespective of their spin-direction). Since we assume no back-scattering from counters to the entangler, the particles which are not counted are lost and hence there is no communication between the two detectors.

3. Derivation of the CH inequality

The basic object for the formulation of the CH inequality is the joint probability $P(Q_1, Q_2)$ for transferring a number of Q_1 and Q_2 electronic charges into leads 1 and 2 over an observation time t . We follow closely the derivation given in [42]. Our starting point is the following algebraic inequality:

$$-1 \leq xy - xy' + x'y + x'y' - x' - y \leq 0, \quad (1)$$

which holds for any variable $0 \leq x, y, x', y' \leq 1$. Let us now introduce explicitly a set of hidden variables τ , which take values in a space \mathcal{T} . We assume that the incoming entangled electron states are described by τ in all the details necessary to determine the probability distributions $P(Q_\alpha, \tau)$ for transferring a number of Q_α electronic charges into lead $\alpha = 1, 2$. By imposing that the hidden variable theory is local, it follows that the joint probability can be expressed in the following form:

$$P(Q_1, Q_2) = \int_{\mathcal{T}} \mathcal{M}(\tau) P(Q_1, \tau) P(Q_2, \tau) d\tau, \quad (2)$$

where $\mathcal{M}(\tau) d\tau$ defines a probability measure on the space \mathcal{T} . The physical meaning of equation (2) is straightforward: it states that the probability distribution on lead α does not depend on the probability distribution on the lead β .

We now introduce $P^{\theta_1, \theta_2}(Q_1, Q_2)$ as the joint probability for transferring Q_1 and Q_2 electronic charges, when both analysers are present, while $P^{\theta_1, -}(Q_1, Q_2)$ and $P^{-, \theta_2}(Q_1, Q_2)$ are the corresponding joint probabilities, when one of the two analysers is removed. If the condition

$$P^{\theta_\alpha}(Q_\alpha, \tau) \leq P(Q_\alpha, \tau) \quad (3)$$

(known as no-enhancement assumption) is verified, it is possible to identify the variables appearing in equation (1) as follows:

$$\begin{aligned} x &= \frac{P^{\theta_1}(Q_1, \tau)}{P(Q_1, \tau)}, & y &= \frac{P^{\theta_2}(Q_2, \tau)}{P(Q_2, \tau)}, \\ x' &= \frac{P^{\theta'_1}(Q_1, \tau)}{P(Q_1, \tau)}, & y' &= \frac{P^{\theta'_2}(Q_2, \tau)}{P(Q_2, \tau)}, \end{aligned} \quad (4)$$

where $P^\theta(Q_\alpha, \tau)$ being the single-terminal probability distribution in the presence of an analyser. Equation (1) can then be rewritten in terms of probabilities, by multiplying each side of the

equation by $P(Q_1, \tau)P(Q_2, \tau)\mathcal{M}(\tau) d\tau$ and integrating over the space \mathcal{T} . Finally, the following inequality is obtained:

$$\begin{aligned} \mathcal{S}_{\text{CH}} = & P^{\theta_1, \theta_2}(Q_1, Q_2) - P^{\theta_1, \theta_2'}(Q_1, Q_2) + P^{\theta_1', \theta_2}(Q_1, Q_2) + P^{\theta_1', \theta_2'}(Q_1, Q_2) \\ & - P^{\theta_1', -}(Q_1, Q_2) - P^{-, \theta_2}(Q_1, Q_2) \leq 0. \end{aligned} \quad (5)$$

Equation (5) is the CH inequality for the full-counting statistics, holding for all values of Q_1 and Q_2 , which satisfy the no-enhancement assumption. We stress that the no-enhancement assumption, upon which equation (5) is based, is not satisfied in general like its optical version. The quantities that we have to compare are probability distributions, so that equation (3) must be checked over the whole range of Q . For a fixed time t and a given mesoscopic system, and hence for a given scattering matrix and incident particle state, the no-enhancement assumption is valid only in some range of values of Q . In particular, different sets of system parameters correspond to different such ranges. The quantity \mathcal{S}_{CH} in equation (5) depends on Q_1 and Q_2 , so that the possible violation, or the extent of it, also depends on Q_1 and Q_2 . Given a certain average number M of entangled pairs that have being injected in the time t , one can look for the maximum violation as a function of the transmitted charges Q_1 and Q_2 .

4. Scattering approach to the full-counting statistics

The joint probabilities appearing in equation (5) can be determined, once the scattering matrix of the mesoscopic conductor is known. The FCS in electronic systems was first introduced by Levitov *et al* [62, 63] in the context of the scattering theory and, later, a Keldysh Green function method [43] to FCS was developed in [44] (for a review see [45]). In this section, we briefly describe how the FCS is formulated for a mesoscopic conductor in the scattering approach. Within this framework, the transport properties of a metallic phase-coherent structure attached to n reservoirs are determined by the matrix S of scattering amplitudes [46]. Such amplitudes are defined through the scattering states describing particles propagating through the leads. For one-dimensional conductors, for example, the scattering state arising from a unitary flux of particles at energy E originating in the i th reservoir reads

$$\varphi_i(x) = \frac{e^{ik_i(E)x} + r_i(E)e^{-ik_i(E)x}}{\sqrt{hv_i(E)}}, \quad (6)$$

for the i th lead, and

$$\varphi_j(x) = \frac{t_{ji}(E)e^{-ik_j(E)x}}{\sqrt{hv_j(E)}}, \quad (7)$$

for the j th lead, with $j \neq i$. Here, $r_i(E)$ is the reflection amplitude for particles at energy E , wave vector $k_i(E)$ and group velocity $v_i(E)$, while $t_{ji}(E)$ is the transmission amplitude from lead i to lead j . Note that $|r_i|^2$, is the probability for a particle to reflect back into the i th lead and $|t_{ji}|^2$ is the probability for the transmission of a particle from lead i to lead j . In the second quantization formalism, a field operator $\hat{\psi}_{j\sigma}(x, t)$ for spin σ particles in lead j is built from scattering states and it is defined as

$$\hat{\psi}_{j\sigma}(x, t) = \int dE \frac{e^{-iEt/\hbar}}{\sqrt{hv_j(E)}} \left[\hat{a}_{j\sigma}(E)e^{ik_j x} + \hat{\phi}_{j\sigma}(E)e^{-ik_j x} \right], \quad (8)$$

where $\hat{a}_{j\sigma}(E)$ ($\hat{\phi}_{j\sigma}(E)$) is the destruction operator for incoming (outgoing) particles at energy E with spin σ in lead j . These operators are linked by the equation

$$\begin{pmatrix} \hat{\phi}_{1\uparrow} \\ \hat{\phi}_{1\downarrow} \\ \hat{\phi}_{2\uparrow} \\ \vdots \end{pmatrix} = S \begin{pmatrix} \hat{a}_{1\uparrow} \\ \hat{a}_{1\downarrow} \\ \hat{a}_{2\uparrow} \\ \vdots \end{pmatrix}, \quad (9)$$

and obey anti-commutation relations

$$\{\hat{a}_{i\sigma}^\dagger(E), \hat{a}_{j\sigma'}(E')\} = \delta_{i,j} \delta_{\sigma,\sigma'} \delta(E - E'). \quad (10)$$

In the case of two- and three-dimensional leads, one can separate longitudinal and transverse particle motion. Since the transverse motion is quantized, the wave function relative to the plane perpendicular to the direction of transport is characterized by a set of quantum numbers, which identifies the channels of the lead. Such channels are referred to as open, when the corresponding longitudinal wave vectors are real, since they correspond to propagating modes. Note that the case of a single open channel corresponds to a one-dimensional lead.

Let us now turn our attention to the probability distribution for the transfer of charges. Following [61], within the scattering approach, the characteristic function of the probability distribution for the transfer of particles in a structure attached to n leads at a given energy E can be written as

$$\chi_E(\vec{\lambda}_\uparrow, \vec{\lambda}_\downarrow) = \left\langle \prod_{j=1,n} e^{i\lambda_{j\uparrow} \hat{N}_I^{j\uparrow}} e^{\lambda_{j\downarrow} \hat{N}_I^{j\downarrow}} \prod_{j=1,n} e^{-i\lambda_{j\uparrow} \hat{N}_O^{j\uparrow}} e^{-i\lambda_{j\downarrow} \hat{N}_O^{j\downarrow}} \right\rangle, \quad (11)$$

where the brackets $\langle \dots \rangle$ stand for the quantum statistical average over the thermal distributions in the leads. Assuming a single channel per lead, $\hat{N}_{I(O)}^{j\sigma}$ is the number operator for incoming (outgoing) particles, with spin σ in lead j and $\vec{\lambda}_\uparrow, \vec{\lambda}_\downarrow$ are vectors of n real numbers, one for each open channel. In terms of incoming and outgoing creation operators, the number operators can be expressed as follows:

$$\hat{N}_I^{j\sigma} = \hat{a}_{j\sigma}^\dagger \hat{a}_{j\sigma}; \quad \hat{N}_O^{j\sigma} = \hat{\phi}_{j\sigma}^\dagger \hat{\phi}_{j\sigma}. \quad (12)$$

Equation (11) can also be recast in the form [62]:

$$\chi_E(\vec{\lambda}_\uparrow, \vec{\lambda}_\downarrow) = \det(\mathbb{I} - n_E + n_E S^\dagger \Lambda^\dagger S \Lambda), \quad (13)$$

where \mathbb{I} is the unit matrix, n_E is the diagonal matrix of Fermi distribution functions $f_j(E)$ for particles in the reservoir j and defined as $(n_E)_{j\sigma,j\sigma} = f_j(E)$, whereas Λ is a diagonal matrix defined as $(\Lambda)_{j\sigma,j\sigma} = \exp(i\lambda_{j\sigma})$. For long measurement times t , the total characteristic function χ is the product of contributions from different energies, so that

$$\chi(\vec{\lambda}_\uparrow, \vec{\lambda}_\downarrow) = \exp \left[\frac{t}{h} \int dE \log \chi_E(\vec{\lambda}_\uparrow, \vec{\lambda}_\downarrow) \right]. \quad (14)$$

At zero temperature, the statistical average over the Fermi distribution function in equation (11) simplifies to the expectation value calculated on the state $|\psi\rangle$, containing two electrons of both

spin species for each channel of a given lead up to the energy corresponding to the chemical potential of such a lead. Furthermore, in the limit of a small bias voltage V applied between the reservoirs, the argument of the integral is energy-independent so that equation (14) can be approximated to

$$\chi(\vec{\lambda}_\uparrow, \vec{\lambda}_\downarrow) \simeq [\chi_0(\vec{\lambda}_\uparrow, \vec{\lambda}_\downarrow)]^M, \quad (15)$$

where only the zero-energy characteristic function appears and $M = eVt/h$ is the average number of injected particles. The joint probability distribution for transferring $Q_{1\sigma}$ spin- σ electrons in lead 1, $Q_{2\sigma}$ spin- σ electrons in lead 2, etc is related to the characteristic function by the relation (we assume that no polarizers are present):

$$P(Q_{1\uparrow}, Q_{1\downarrow}, Q_{2\uparrow}, \dots) = \frac{1}{(2\pi)^{2n}} \int_{-\pi}^{+\pi} d\lambda_{1\uparrow} d\lambda_{1\downarrow} d\lambda_{2\uparrow} \dots \chi(\vec{\lambda}_\uparrow, \vec{\lambda}_\downarrow) e^{i\vec{\lambda}_\uparrow \cdot \vec{Q}_\uparrow} e^{i\vec{\lambda}_\downarrow \cdot \vec{Q}_\downarrow}. \quad (16)$$

In the rest of the paper, we shall consider systems with two counting terminals only. In particular, while the counting terminals are kept at zero chemical potential, all other terminals are biased at chemical potential eV . For later convenience, we write down the most general expression for the characteristic function, when spin- σ electrons are counted in lead 1 and spin- σ' electrons are counted in lead 2:

$$\chi_E(\lambda_{1\sigma}, \lambda_{2\sigma'}) = 1 + (e^{-i\lambda_{1\sigma}} - 1) \langle \hat{N}_O^{1\sigma} \rangle + (e^{-i\lambda_{2\sigma'}} - 1) \langle \hat{N}_O^{2\sigma'} \rangle + (e^{-i\lambda_{1\sigma}} - 1)(e^{-i\lambda_{2\sigma'}} - 1) \langle \hat{N}_O^{1\sigma} \hat{N}_O^{2\sigma'} \rangle, \quad (17)$$

in the relevant energy range $0 < E < eV$.

5. Entangled electrons

We shall now test the inequality presented in equation (5) in an ideal situation in which the entangled pair is generated by some entangler in the same spirit as in [32, 33]. In section 6, we shall analyse the effect of decoherence and in section 7, we shall demonstrate that a normal beam-splitter, in the absence of interaction, constitutes a simple realization of an entangler.

In the setup depicted in figure 1, we assume the existence of an entangler that produces electron pairs in the Bell state

$$|\psi_B\rangle = \frac{1}{\sqrt{2}} [a_{3\uparrow}^\dagger(E) a_{4\downarrow}^\dagger(E) \pm a_{3\downarrow}^\dagger(E) a_{4\uparrow}^\dagger(E)] |0\rangle, \quad (18)$$

of spin triplet (upper sign) or spin singlet (lower sign) in the energy range $0 < E < eV$. These electrons propagate through the conductors, which connect terminals 3 and 4 with leads 1 and 2, as though terminals 3 and 4 were kept at a potential eV with respect to 1 and 2. Our aim is to test the violation of the CH inequality given in equation (5) for such maximally entangled states.

When the angles θ_1 and θ_2 are parallel to each other, the scattering matrix of the two conductors, in the absence of spin-mixing processes, can be written as

$$\bar{S} = \begin{pmatrix} \hat{S}_{13} & 0 \\ 0 & \hat{S}_{24} \end{pmatrix}, \quad (19)$$

where

$$\hat{S}_{13} = \begin{pmatrix} \check{r}_3 & \check{t}_{31} \\ \check{t}_{13} & \check{r}_1 \end{pmatrix} = \begin{pmatrix} r_{3\uparrow} & 0 & t_{31\uparrow} & 0 \\ 0 & r_{3\downarrow} & 0 & t_{31\downarrow} \\ t_{13\uparrow} & 0 & r_{1\uparrow} & 0 \\ 0 & t_{13\downarrow} & 0 & r_{1\downarrow} \end{pmatrix}. \quad (20)$$

Here, $r_{j\sigma}$ ($t_{ij\sigma}$) is the probability amplitude for an incoming particle, with spin σ from lead j to be reflected (transmitted in lead i). For a normal-metallic wire, we set $t_{ij\uparrow} = t_{ij\downarrow} = \sqrt{T}$, $t_{ji\uparrow} = t_{ji\downarrow} = \sqrt{T}$ and $r_{j\uparrow} = r_{j\downarrow} = i\sqrt{1-T}$, where T is the transmission probability. The expression for \hat{S}_{24} is written analogously. For simplicity, we will assume that \hat{S}_{13} and \hat{S}_{24} are equal. The general scattering matrix relative to non-collinear angles is obtained from \bar{S} by rotating the spin-quantization axis independently in the two conductors (note that this is possible, because the two wires are decoupled). The ‘rotated’ S-matrix is obtained [60] by the transformation $\bar{S}_{\theta_1, \theta_2} = \bar{U} \bar{S} \bar{U}^\dagger$, where \bar{U} is the rotation matrix given by

$$\bar{U} = \begin{pmatrix} \check{U}_{\theta_1} & 0 & 0 & 0 \\ 0 & \check{1} & 0 & 0 \\ 0 & 0 & \check{U}_{\theta_2} & 0 \\ 0 & 0 & 0 & \check{1} \end{pmatrix}, \quad (21)$$

where

$$\check{U}_\theta = \begin{pmatrix} \cos \frac{\theta}{2} & \sin \frac{\theta}{2} \\ -\sin \frac{\theta}{2} & \cos \frac{\theta}{2} \end{pmatrix}. \quad (22)$$

The probability distributions are now given by the expression in equation (16), where the expectation value is performed over the state $|\psi\rangle$ given by equation (18). In the case where both analysers are present, we set $\sigma = \sigma' = \uparrow$. The probability distribution, when one of the analysers are removed, for example the upper one in figure 1, is obtained by replacing $\hat{N}_O^{1\sigma}$ with $\hat{N}_O^{1\uparrow} + \hat{N}_O^{1\downarrow}$ and $\hat{N}_O^{2\sigma'}$ with $\hat{N}_O^{2\uparrow}$.

For the single-terminal probability distributions in leads $i = 1, 2$ we get, in the presence and in the absence of an analyser, respectively,

$$P^{\theta_i}(Q_i) = \binom{M}{Q_i} \left(\frac{T}{2}\right)^{Q_i} \left(1 - \frac{T}{2}\right)^{M-Q_i} \quad (23)$$

$$P(Q_i) = \binom{M}{Q_i} (T)^{Q_i} (1 - T)^{M-Q_i}, \quad (24)$$

so that the no-enhancement assumption reads:

$$\left(1 - \frac{T}{2}\right)^{(M-Q_i)} \left(\frac{1}{2}\right)^{Q_i} \leq (1 - T)^{(M-Q_i)}, \quad i = 1, 2. \quad (25)$$

Note that the probabilities in equations (23) and (24) do not depend on the angles θ_1 and θ_2 , because the expectation value of the operator $\hat{N}_O^{i\sigma}$ is invariant under spin rotation. As a consequence, the effect of the analyser is equivalent to a reduction of the transmission probability T by a factor of 2, resulting in a shift of the maximum of the distribution. From equation (25) it follows that, for a given number $M = eVt/h$ of entangled pairs generated by the entangler, the ‘no-enhancement’ assumption holds only for certain values of T and Q_i . Thus the CH inequality of equation (5) can be tested for violation only for appropriate values of M , T and Q_1 or Q_2 . For example, for a given observation time t (i.e. a given M) and a given value of Q , the CH inequality can be tested only for transmission T less than a maximum value given by the expression,

$$T_{\max} = \frac{2^{\frac{Q_i}{M-Q_i}} - 1}{2^{\frac{Q_i}{M-Q_i}} - \frac{1}{2}}. \quad (26)$$

At the edge of the distribution ($Q_i = M$), the no-enhancement assumption is satisfied for every T . The window of allowed Q_i values where the no-enhancement assumption is satisfied gets wider on approaching the tunneling limit. For large M , $T_{\max} \simeq 2(\log 2)\frac{Q_i}{M}$. The previous inequality can also be interpreted as a limit for the allowed measuring time given a setup at disposal. Alternatively, given a certain transmission, the no-enhancement assumption is verified for points of the distribution such that:

$$\frac{Q_i}{M} \geq \frac{\log \frac{1-T/2}{1-T}}{\log 2 + \log \frac{1-T/2}{1-T}}. \quad (27)$$

The various probabilities needed to define \mathcal{S}_{CH} are reported in [37]. Let us now analyse the possibility of violation of the CH inequality. First consider the situation where the entangler emits a single entangled pair of electrons, in which case $P^{\theta_1, \theta_2}(1, 1) = \langle \psi | \hat{N}_O^{1\uparrow} \hat{N}_O^{2\uparrow} | \psi \rangle$, $P^{-, \theta_2}(1, 1) = \langle \psi | (\hat{N}_O^{1\uparrow} + \hat{N}_O^{1\downarrow}) \hat{N}_O^{2\uparrow} | \psi \rangle$ and $P^{\theta_1, -}(1, 1) = \langle \psi | \hat{N}_O^{1\uparrow} (\hat{N}_O^{2\uparrow} + \hat{N}_O^{2\downarrow}) | \psi \rangle$. We find that the CH inequality is maximally violated for the following choice of angles: $\theta_2 - \theta_1 = \theta'_2 - \theta'_1 = 3\pi/4$. More precisely we obtain:

$$\mathcal{S}_{\text{CH}} = T^2 \frac{\sqrt{2} - 1}{2}, \quad (28)$$

which is equal to the result obtained for an entangled pair of photons [42], where T plays the role of the quantum efficiency of the photon detectors. In the more general case of $Q_1 = Q_2 = M$, for $M \gg 1$, we have

$$P^{\theta_1, \theta_2}(M, M) = \frac{T^{2M}}{2^M} \left[\sin^2 \left(\frac{\theta_1 \pm \theta_2}{2} \right) \right]^M, \quad (29)$$

$$P^{\theta_1, -}(M, M) = P^{-, \theta_2}(M, M) = \frac{T^{2M}}{2^M},$$

so that the no-enhancement assumption is always satisfied and the quantity \mathcal{S}_{CH} can be easily evaluated:

$$\mathcal{S}_{\text{CH}} = \frac{T^{2M}}{2^M} \left[\sin^{2M} \frac{\theta_1 \pm \theta_2}{2} - \sin^{2M} \frac{\theta_1 \pm \theta'_2}{2} + \sin^{2M} \frac{\theta'_1 \pm \theta_2}{2} + \sin^{2M} \frac{\theta'_1 \pm \theta'_2}{2} - 2 \right]. \quad (30)$$

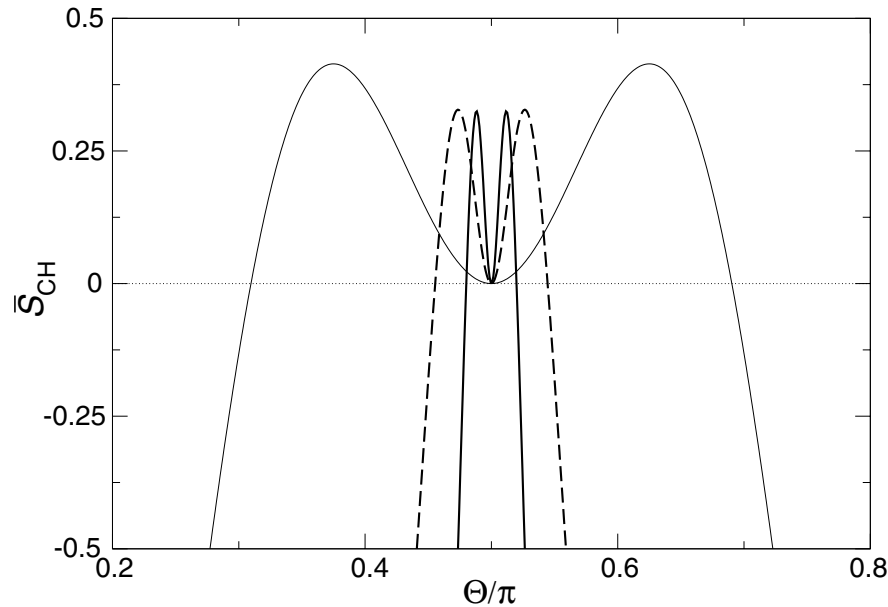


Figure 2. The quantity $\bar{\mathcal{S}}_{\text{CH}} = \mathcal{S}_{\text{CH}}/(T^{2M}/2^M)$ is plotted as a function of the angle Θ for different numbers of injected entangled pairs by the entangler: $M = 1$ (thin solid line), $M = 20$ (thick broken line) and $M = 100$ (thick solid line). The range of angles relative to positive values shrinks with increasing M , while the value of the maximum slightly decreases.

The rotational invariance makes $P^{\theta_1,-}$ and P^{-,θ_2} independent of angles, and P^{θ_1,θ_2} dependent on the angles through $\frac{\theta_1 \pm \theta_2}{2}$. This allows us, without loss of generality, to define an angle Θ , such that $2\Theta = \theta_1 \pm \theta_2 = \theta'_1 \pm \theta_2 = \theta'_1 \pm \theta'_2 = (\theta_1 \pm \theta_2)/3$. As a result, equation (5) takes the form:

$$\mathcal{S}_{\text{CH}} = 3P_{1,2}^{\Theta}(Q_1, Q_2) - P_{1,2}^{3\Theta}(Q_1, Q_2) - P_{1,-}(Q_1, Q_2) - P_{-,2}(Q_1, Q_2) \leq 0, \quad (31)$$

where $P_{1,2}^{\Theta} = P^{\theta_1,\theta_2}$ and $P_{1,-} = P^{\theta_1,-}$. It is useful to define the reduced quantity $\bar{\mathcal{S}}_{\text{CH}} = \mathcal{S}_{\text{CH}}/(T^{2M}/2^M)$, which is plotted in figure 2 as a function of Θ for different values of M (note that since $P^{\theta_1,-}(M, M) = (T^{2M}/2^M)$, $\bar{\mathcal{S}}_{\text{CH}}$ is nothing but $\mathcal{S}_{\text{CH}}/P^{\theta_1,-}(M, M)$). The violation occurs for every value of M in a range of angles around $\Theta = \pi/2$ (note that \mathcal{S}_{CH} is symmetric with respect to $\pi/2$). The range of angles for which $\bar{\mathcal{S}}_{\text{CH}}$ is positive shrinks with increasing M , while the maximum value of $\bar{\mathcal{S}}_{\text{CH}}$ decreases very weakly with M (more precisely, $\bar{\mathcal{S}}_{\text{CH}}^{\text{max}} \propto 1/M$). This means that the effect of the factor $T^{2M}/2^M$ on the value of \mathcal{S}_{CH} is exponentially strong, making the violation of the CH inequality exponentially difficult to detect for large M and $Q_1 = Q_2 = M$. The weakening of the violation is mainly due to the suppression of the joint probabilities. As we shall show later, by optimizing all the parameters, it is yet possible to eliminate this exponential suppression.

Let us now consider the violation of the CH inequality as a function of the transmitted charges. We notice that, for large M , the CH inequality is not violated for the off-diagonal terms of the distributions (when $Q_1 \neq Q_2$), meaning that one really needs to look at ‘coincidences’. Therefore, we discuss the case $Q_1 = Q_2 \equiv Q < M$ (remember that the no-enhancement assumption is satisfied only for $T \leq T_{\text{max}}(Q)$). We find that the maximum violation, for a given

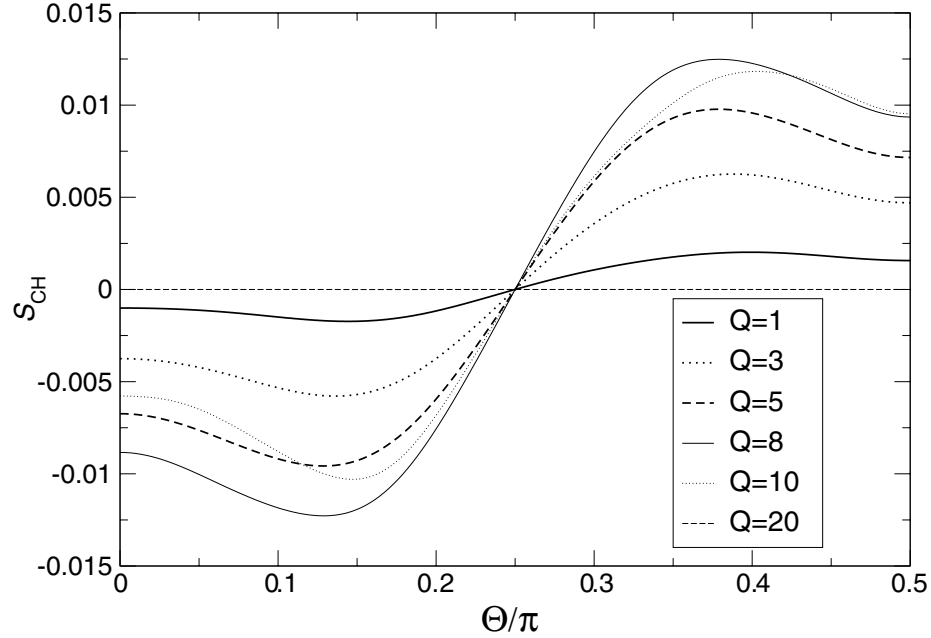


Figure 3. The quantity \mathcal{S}_{CH} is plotted as a function of the angle Θ for $M = 20$ and T set to the highest value allowed by the no-enhancement assumption, different for each Q . The curves are relative to different values of $Q = [1, 20]$. The maximum of \mathcal{S}_{CH} increases with Q reaching its largest value for $Q = 8$ and decreasing for $Q > 8$. Note that the variation of \mathcal{S}_{CH} with Θ for $Q = 20$ is not appreciable on this scale.

M and Q , always occurs at $T = T_{\text{max}}$. In order to get the largest violation of the CH inequality at a given M and Q one could, in principle, choose the highest allowed value of T for each value of Q ($T = T_{\text{max}}(Q)$). In figure 3, we plot the quantity \mathcal{S}_{CH} for $M = 20$ as a function of Θ and different values of Q . For every $Q < M$, the violation occurs in the same range of angles, namely $\pi/4 \leq \Theta \leq \pi/2$, because of the following properties of the joint probability distributions: $P_{1,2}^{\Theta}(Q_1, Q_2) = P_{1,2}^{3\Theta}(Q_1, Q_2) = P_{1,-}(Q_1, Q_2)$ for $\Theta = \pi/4$. This implies that $\mathcal{S}_{\text{CH}}(\Theta = \pi/4) = 0$, and $P_{1,2}^{\Theta}(Q_1, Q_2) \geq P_{1,2}^{3\Theta}(Q_1, Q_2), P_{1,-}(Q_1, Q_2), P_{-,2}^{\Theta}(Q_1, Q_2)$ for $\pi/4 \leq \Theta \leq \pi/2$. Furthermore, in this specific case of $M = 20$, we find that the maximum values of \mathcal{S}_{CH} occurs at $Q = 8$.

In figure 4, we plot the maximum value of \mathcal{S}_{CH} , with respect to Θ and T , as a function of Q for different values of M . Several observations are in order. For increasing M , the position of the maximum Q_{max} is very weakly dependent on M . Remarkably, the value of the maximum of the curves does not decrease exponentially, but rather as $1/M$. Despite the exponential suppression of the joint probability with M , the extent of the maximal violation scales with M much slowly (polynomially).

If the entangler is substituted with a source that emits factorized states, the CH inequality given in equation (5) is never violated. In this case, in contrast to equation (18), the state emitted by the source reads: $|\psi\rangle = a_{3\uparrow}^{\dagger} a_{3\downarrow}^{\dagger} a_{4\uparrow}^{\dagger} a_{4\downarrow}^{\dagger} |0\rangle$. All the previous calculations can be repeated and we find, as expected, that the characteristic functions factorize, so that the two-terminal joint probability distributions are given by the product of the single-terminal probability distributions.

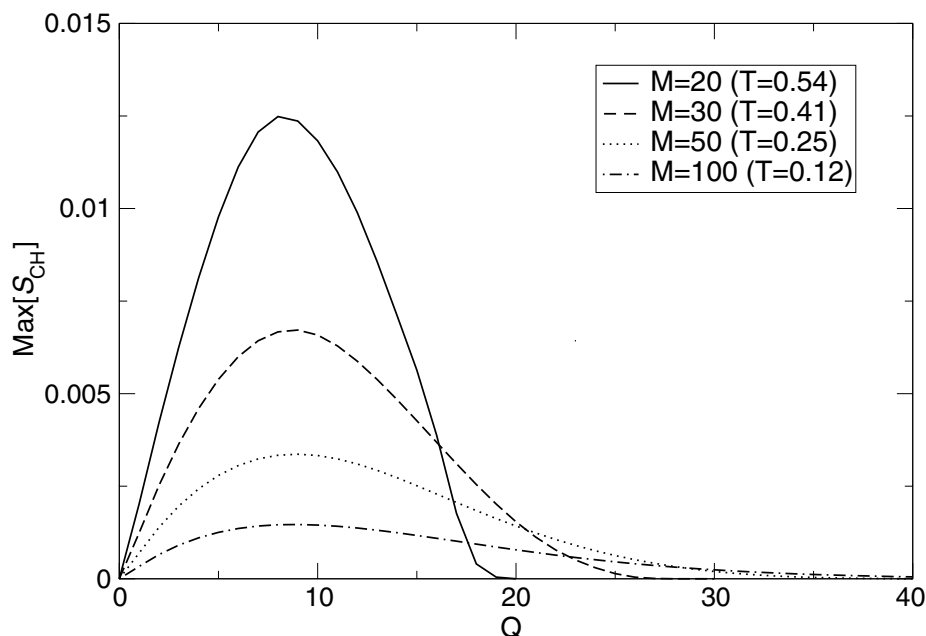


Figure 4. The maximum value of the quantity S_{CH} , evaluated over angles Θ and transmission probabilities T , is plotted as a function of Q . The curves are relative to different values of M ranging from 20 to 100. In the legend box is indicated the value of transmission T corresponding to the maximum of the curves.

To conclude, we wish to mention that the CH inequality (equation (5)) holds for joint probabilities relative to arbitrary observation time, although the FCS requires a long observation time, so that $M \gg 1$.

6. Effect of dephasing

In real systems, at finite temperature, electrons interact among themselves, with the lattice phonons and furthermore, are unavoidably coupled to the electromagnetic environment. As a result, dephasing takes place, reducing or destroying entanglement. The evaluation of the effects of dephasing on entangled electrons is an important issue discussed in the literature as follows. In [11, 14, 27, 38] dephasing was modelled in terms of a density matrix, whose off-diagonal elements, which give rise to the entanglement, are suppressed by a phenomenological parameter. By properly choosing the transmission probability of beam-splitters, or tunnel barriers, violation of Bell inequality was found even for strong dephasing. In [23, 39] dephasing was introduced by averaging over a uniform distribution of random phase factors accumulated in each edge channel of the quantum Hall bar. If the two edge channels are mixed by the tunnel barrier, no violation is reported for strong dephasing. The effect of decoherence and relaxation has also been analysed using a Bloch equation formalism in [40].

We consider the situation where decoherence is produced by inelastic processes occurring in the wires due to the presence of additional fictitious leads [58]. Various phenomenological methods have been developed, in general, to treat dephasing in transport through mesoscopic conductors. In [53, 54], which actually describe exactly the nonequilibrium radiation acting on

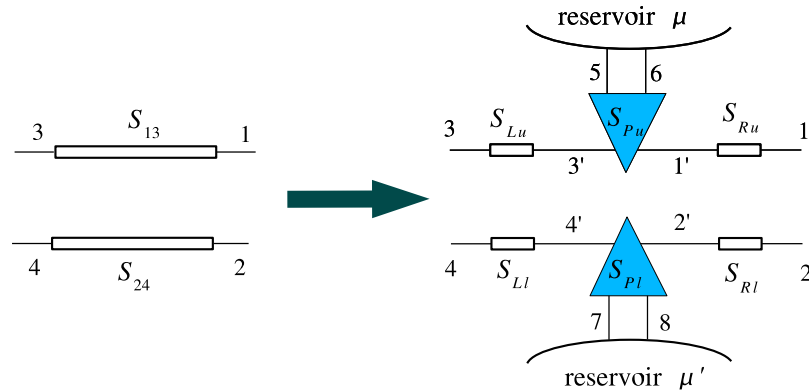


Figure 5. Decoherence is introduced by including the effect of an additional fictitious reservoir. Each wire is therefore replaced with a structure composed of three parts. For the upper (lower) wire they are: an elastic scatterer characterized by the S-matrix S_{Lu} (S_{Ll}), an element which provides the coupling to the additional reservoir of chemical potential μ (μ') and characterized by the matrix S_{Pu} (S_{Pl}), and finally another elastic scatterer S_{Ru} (S_{Rl}).

the system, dephasing is induced by a fluctuating classical potential. In [55], dephasing is treated as random fluctuations of the phase of propagating modes through the conductor. Both methods have been recently applied to FCS [56, 57]. The advantage of the fictitious lead model resides in the fact that inelastic, phase-randomization processes are implemented within an elastic, time-independent scattering problem.

Each conductor in figure 1 is replaced by a structure composed of three scattering regions, as shown in figure 5. In the upper wire, due to the presence of the additional reservoir, particles propagating through lead 3 are transmitted partially to lead 1 and partially to leads 5 and 6 (see figure 5). The additional reservoir, however, can transfer itself particles to leads 1 and 3. As a result, only a fraction of the particles arriving in lead 1 comes from coherently transmitted ones sent in from lead 3, with probability

$$T_{13} = \frac{T_0^2(1 - \alpha)}{[1 + (1 - T_0)(1 - \alpha)]^2}. \quad (32)$$

Another fraction, the incoherent contribution, comes from the additional reservoir through leads 5 and 6, with probability

$$T_{15} + T_{16} = \frac{T_0\alpha}{1 + (1 - T_0)(1 - \alpha)}. \quad (33)$$

This mimics the fact that the current flowing through the conductor is partially composed of particles (the incoherent fraction) which have lost phase memory while traversing it. For $\alpha = 0$, all particles are coherently transmitted and $T_{15} + T_{16} = 0$, while for $\alpha = 1$, all particles are transferred incoherently and $T_{13} = 0$. Note that one has to include two channels that couple to the additional reservoir in order to allow for complete phase randomization ($T_{13} = 0$). A similar description applies to the lower wire connecting lead 4 with lead 2. For $\alpha = 0$, the overall transmission probability through the conductors is given by $T = T_0^2/(2 - T_0)^2$. In what

follows we will also refer to α as the decoherence rate. The chemical potentials μ and μ' of the additional reservoirs are set in such a way that no net current flows in or out of the reservoirs. More precisely, we impose $I_5 + I_6 = 0$ and $I_7 + I_8 = 0$, where I_i is the average current flowing in lead i . On average, therefore, every electron that escapes the wires through the additional leads is returned by another one with loss of phase memory. An instantaneous current through leads 5, 6, 7 and 8 is then allowed, and a non-fluctuating chemical potential μ is assumed [48, 51, 52]. For simplicity, we shall assume that $\hat{S}_{Ru} = \hat{S}_{Lu}$ and $\hat{S}_{Li} = \hat{S}_{Ri}$ and furthermore that the two conductors are equal, i.e. $\hat{S}_{13} = \hat{S}_{24}$, and subjected to the same degree of decoherence. From this follows that $\mu = \mu'$.

In the symmetrical setup, we are considering here $\mu = eV/2$, so that, at zero temperature, the initial state of the system $|\psi\rangle$ takes different forms depending on whether the energy of electrons falls within the range $E < \mu$ or $\mu < E < eV$. Namely,

$$|\psi\rangle = \begin{cases} |\psi_B\rangle, & \mu < E < eV, \\ |\psi_S\rangle, & E < \mu, \end{cases} \quad (34)$$

where $|\psi_B\rangle$, is defined in equation (18) and

$$|\psi_S\rangle = \frac{1}{\sqrt{2}} [a_{3\uparrow}^\dagger(E)a_{4\downarrow}^\dagger(E) \pm a_{3\downarrow}^\dagger(E)a_{4\uparrow}^\dagger(E)] \prod_{n=5,6,7,8} a_{n\uparrow}^\dagger(E)a_{n\downarrow}^\dagger(E) |0\rangle. \quad (35)$$

Note that, in the presence of decoherence ($\alpha \neq 0$), for $E < \mu$ particles are arriving both from the entangler and from the additional reservoir.

When the fictitious lead is present, the interval of integration in equation (14) can be separated into two energy ranges, namely $E < \mu$ and $\mu < E < eV$. Since in the limit of a small voltage bias V , χ_E is energy-independent, equation (14) can be approximated to

$$\chi(\vec{\lambda}_\uparrow, \vec{\lambda}_\downarrow) \simeq [\chi_0^S(\vec{\lambda}_\uparrow, \vec{\lambda}_\downarrow)]^{M_\mu} [\chi_0^B(\vec{\lambda}_\uparrow, \vec{\lambda}_\downarrow)]^{M-M_\mu}, \quad (36)$$

where $\chi_0^{S(B)}$ is calculated over the state $|\psi_{S(B)}\rangle$, $M_\mu = \mu t/h$ and $M = eVt/h$. According to equation (16), both single terminal and joint probability distributions require the computation of multidimensional integrals of complex expressions. In [47], it is shown that the various probability distributions needed to evaluate the CH inequality can be expressed in a differential form, which is more suitable for numerical evaluation. As for the case of no-decoherence, the rotational invariance makes $P^{\theta_1, -\theta_2}(Q_1, Q_2)$ and $P^{-\theta_1, \theta_2}(Q_1, Q_2)$ independent of angles and factorizable, while it makes $P^{\theta_1, \theta_2}(Q_1, Q_2)$ dependent on the angles through $\frac{\theta_1 \pm \theta_2}{2}$, so that the CH inequality can still be written as in equation (31), with $\Theta = \frac{\theta_1 \pm \theta_2}{2}$.

Let us first analyse the effect of decoherence on the no-enhancement assumption, equation (3). For a given number of transmitted particles Q either in lead 1 or 2, single-terminal probabilities, with or without analyser, depend on α , M and T . As in the absence of decoherence, it turns out that for a given α , M and Q , the no-enhancement assumption is satisfied only for a range of values of the transmission T smaller or equal to a certain upper bound $T_{\max}(\alpha, M, Q)$. For $\alpha \neq 0$, however, it is not possible to find an analytical expression for T_{\max} . In figure 6, T_{\max} is plotted as a function of α for $M = 30$ and several values of Q from 1 to 22. One can see that T_{\max} monotonically decreases with α for values of $Q \lesssim M/2$ and monotonically increases for bigger values of Q . This means that, for small values of Q , decoherence restricts

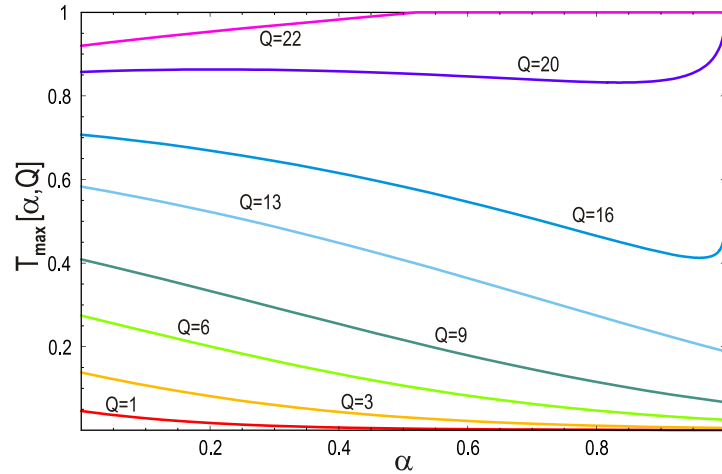


Figure 6. Maximum value of the wire transmission T_{\max} allowed by the no-enhancement assumption as a function of decoherence rate α for $M = 30$ emitted pairs and for the different values of Q .

the applicability of the CH inequality (see [47] for a thorough discussion). Since the CH inequality involves probability distributions in both leads 1 and 2, the no-enhancement assumption must be satisfied in each arm. If we consider different numbers of transmitted particles in leads 1 and 2 ($Q_1 \neq Q_2$), the maximum allowed transmission probability must be taken to be the minimum between $T_{\max}(\alpha, M, Q_1)$ and $T_{\max}(\alpha, M, Q_2)$, according to our assumption of identical wires. We therefore define

$$T_{\max}(\alpha, M, Q_1, Q_2) = \text{Min}[T_{\max}(\alpha, M, Q_1), T_{\max}(\alpha, M, Q_2)]. \quad (37)$$

Let us now move to the effects of decoherence on the violation of the CH inequality. There are two general characteristics of the behaviour of \mathcal{S}_{CH} that were already found in the absence of decoherence and that still hold for finite α :

- for given M , Q_1 and Q_2 the maximum violation always occurs for $T = T_{\max}(\alpha, M, Q_1, Q_2)$;
- there is always an angle for which \mathcal{S}_{CH} is maximum, which we shall denote by $\Theta_{\text{best}}(\alpha, M, Q_1, Q_2)$.

Let us now analyse the maximum violation of the CH inequality for a given M with $T = T_{\max}$ and $\Theta = \Theta_{\text{best}}$ as a function of $Q \equiv Q_1 = Q_2$ and for different values of α . In figure 7, the four curves are relative to $\alpha = 0, 0.3, 0.5$ and 0.8 and $M = 30$. Several observations are in order. For a given value of Q , violation is always larger in the absence of decoherence and decreases as α increases. If we denote with Q_{best} the position of the maximum of a curve, for all values of decoherence rate $Q_{\text{best}} \sim M/3$. Note furthermore that, as decoherence gets stronger, the range of values of Q for which violation takes place shrinks.

To conclude we add that, if the entangler is substituted with a source that emits factorized states, the CH inequality is never violated for any decoherence rate. This is simply due to the fact that two-terminal joint probability distributions are given by the product of single-terminal probability distributions, thus making the CH inequality always equal to zero.

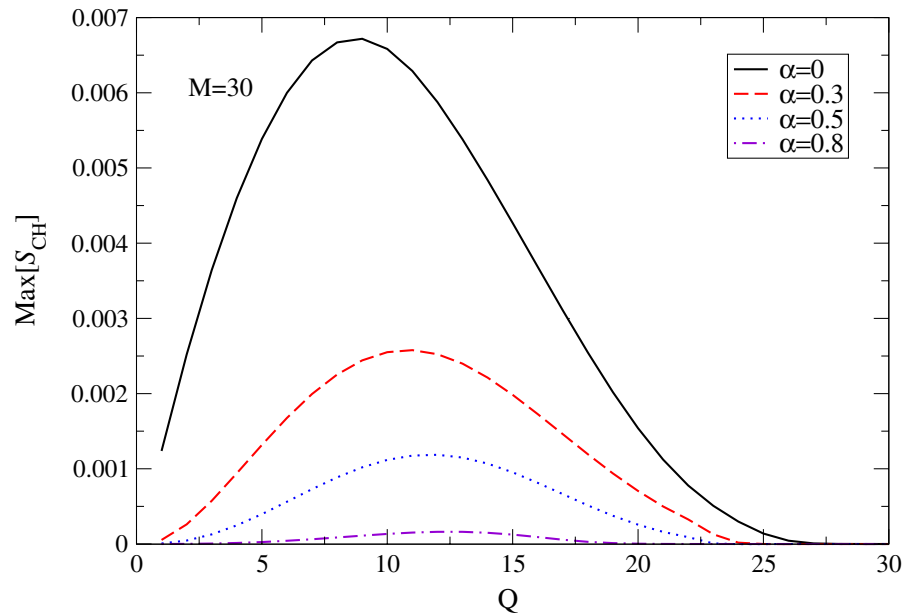


Figure 7. Maximum value of the quantity \mathcal{S}_{CH} (in $T = T_{\max}$ and $\Theta = \Theta_{\text{best}}$) as a function of Q for $M = 30$ and different values of decoherence: $\alpha = 0, 0.3, 0.5$ and 0.8 . The largest violation always occurs in the absence of decoherence and, for a given Q , violation is reduced monotonically with α . The position where the maximum occurs, Q_{best} , slightly increases with α .

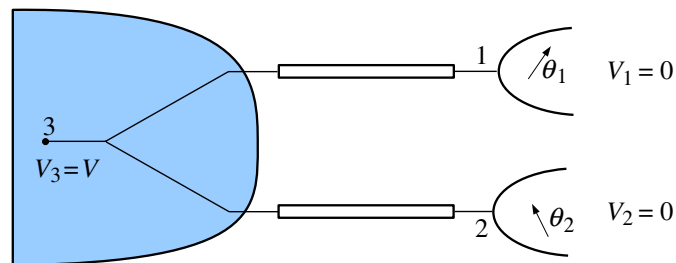


Figure 8. Setup of a realistic system consisting of a normal beam-splitter (shaded region) for testing the CH inequality. Bold lines represent two conductors of unit transmission probability. A bias voltage equal to eV is set between terminals 3 and 1 and terminals 3 and 2.

7. Normal beam-splitter

We are now ready to analyse realistic structures by discussing the CH inequality along the lines of section 5. To this aim, we consider a normal beam-splitter (shaded block in figure 8) in which lead 3 is kept at a potential eV and leads 1 and 2 are grounded, so that the same bias voltage is established between 3 and 1, and 3 and 2. The two conductors, which connect the beam-splitter to the leads 1 and 2, are assumed to be normal-metallic and perfectly transmissive, so that the S-matrix of the system for $\theta_1 = \theta_2 = 0$ is equal to the S-matrix of the beam-splitter, which

reads [58]

$$S = \begin{pmatrix} -(a+b) & \sqrt{\epsilon} & \sqrt{\epsilon} \\ \sqrt{\epsilon} & a & b \\ \sqrt{\epsilon} & b & a \end{pmatrix}. \quad (38)$$

In this parametrization of a symmetric beam-splitter $a = \pm(1 + \sqrt{1 - 2\epsilon})/2$, $b = \mp(1 - \sqrt{1 - 2\epsilon})/2$ and $0 < \epsilon < 1/2$. For arbitrary angles θ_1 and θ_2 , the S-matrix is obtained by rotating the quantization axis in the two conductors independently by applying the transformation $S_{\theta_1, \theta_2} = \mathcal{U} S \mathcal{U}^\dagger$, where \mathcal{U} is the rotation matrix given by

$$\mathcal{U} = \begin{pmatrix} \check{1} & 0 & 0 \\ 0 & \check{U}_{\theta_1} & 0 \\ 0 & 0 & \check{U}_{\theta_2} \end{pmatrix} \quad (39)$$

and \check{U}_θ is defined in equation (22). This procedure is valid as long as no back-scattering is present in the conductors. The probability distributions are given by equation (16), where the state $|\psi\rangle$ is now factorizable

$$|\psi\rangle = a_{3\uparrow}^\dagger(E) a_{3\downarrow}^\dagger(E) |0\rangle, \quad (40)$$

in the energy range $0 < E < eV$. Analogously to what was done in section 5, when both analysers are present, we set $\sigma = \sigma' = \uparrow$. For the expectation values we get:

$$\langle \psi | \hat{N}_O^{1\uparrow} | \psi \rangle = \langle \psi | \hat{N}_O^{2\uparrow} | \psi \rangle = \epsilon, \quad (41)$$

$$\langle \psi | \hat{N}_O^{1\downarrow} | \psi \rangle = \epsilon, \quad (42)$$

$$\langle \psi | \hat{N}_O^{1\uparrow} \hat{N}_O^{2\uparrow} | \psi \rangle = \epsilon^2 \sin^2 \left(\frac{\theta_1 - \theta_2}{2} \right) \quad (43)$$

and

$$\langle \psi | \hat{N}_O^{1\downarrow} \hat{N}_O^{2\uparrow} | \psi \rangle = \epsilon^2 \cos^2 \left(\frac{\theta_1 - \theta_2}{2} \right), \quad (44)$$

obtaining the joint-probability distributions reported in [37]. The above number operator expectation values are equal to the case of the entangler, when ϵ is replaced by $T/2$, whereas the cross-terminal correlators are equal in the two cases, if ϵ is replaced with $T/\sqrt{2}$. From this it follows that the characteristic functions for the beam-splitter possess the same dependence on the angle difference as the corresponding characteristic functions for the entangler (section 5), but have a different structure as far as scattering probabilities are concerned. In particular, as expected [62], the cross-correlations vanish, when the two angles are equal. In contrast, when the angle difference is π , cross-correlations are maximized. Furthermore, when only one analyser is present the characteristic function shows no dependence on the angle, but it is not factorizable, in contrast to the case of the entangler. As a result, the single-terminal probabilities, given by equation (16), are equal in the two cases, provided that ϵ is replaced with $T/2$. The joint

probabilities for $Q_1 = Q_2 = M$ are equal in the two cases, if ϵ is replaced with $T/\sqrt{2}$ (however, this replacement is not valid in general for joint probabilities with $Q_1, Q_2 \neq M$):

$$P^{\theta_1, \theta_2}(M, M) = \left[\epsilon^2 \sin^2 \left(\frac{\theta_1 - \theta_2}{2} \right) \right]^M, \quad (45)$$

$$P^{\theta_1, -}(M, M) = \epsilon^{2M}. \quad (46)$$

The no-enhancement assumption is verified when

$$\epsilon \leq \frac{1}{2} \frac{2^{\frac{Q}{M-Q}} - 1}{2^{\frac{Q}{M-Q}} - \frac{1}{2}}, \quad (47)$$

which equals the condition of equation (26), once ϵ is replaced with $T/2$. Let us first consider the case for which $Q_1 = Q_2 = M$. We obtain an important result: the CH inequality is violated for the same set of angles found for the case of the entangler, although to a lesser extent, since the prefactors in equations (45) and (46) now vary in the range $0 \leq \epsilon^{2M} \leq \frac{1}{4^M}$. In particular, in the simplest case of $M = 1$, corresponding to injecting a single pair of electrons, the maximum violation corresponds to $\mathcal{S}_{\text{CH}} = \frac{\sqrt{2}-1}{4}$, which is a half of the value for the entangler. Furthermore, the plot in figure 2 is also valid in the present case with $\bar{\mathcal{S}}_{\text{CH}}$ defined as $\bar{\mathcal{S}}_{\text{CH}} = \mathcal{S}_{\text{CH}}/\epsilon^{2M}$, i.e. by replacing $T/\sqrt{2}$ with ϵ . This means that a geometry like that of the beam-splitter enables one to detect violation of the CH inequality without any need to resort to interaction processes to extract entanglement.

Also here, we consider the case for which $Q_1 = Q_2 \equiv Q < M$, where interesting differences with respect to the case of the entangler are found. (i) We find that the violation of the CH inequality is in general weaker, meaning that the absolute maximum value of \mathcal{S}_{CH} is smaller than in the ideal case of the entangler. (ii) The weakening of the violation with increasing M is determined by the suppression of the probability by the prefactor $(\epsilon^2)^{Q_1+Q_2}$. Remarkably, the maximum value of \mathcal{S}_{max} decreases like $1/M$, therefore even slower than for the ideal case. (iii) Violations occur only for values of Q close to 1, even for large values of M : to search for violations one has to look at single- or few-pair probabilities and therefore, because of the no-enhancement assumption, to small transmissions ϵ . (iv) Interestingly, for $Q = 1$, the quantity \mathcal{S}_{CH} is positive for any angle, although the largest values correspond to Θ close to $\pi/2$. We do not find any relevant variation, with respect to the discussion in section 5, for probabilities relative to $Q_1 \neq Q_2$.

It is easy to convince oneself that, for an incident state composed of a single pair of particles impinging from the entering arm of the beam-splitter (40), we obtain a final state

$$|\psi\rangle_{\text{out}} = \epsilon (b_{1\uparrow}^\dagger b_{2\downarrow}^\dagger - b_{1\downarrow}^\dagger b_{2\uparrow}^\dagger) |0\rangle + \epsilon b_{1\uparrow}^\dagger b_{1\downarrow}^\dagger |0\rangle + \epsilon b_{2\uparrow}^\dagger b_{2\downarrow}^\dagger |0\rangle, \quad (48)$$

that contains an entangled part which gets post-selected by the measurement. In [64], this fact was already noticed. In the limit of a strongly asymmetric beam-splitter, the state (48) is analogous to the one discussed in [23]. For mesoscopic conductors, entanglement without interaction for electrons injected from a Fermi sea has been discussed in [21], [23]–[30], [37, 39].

8. Conclusions

In this paper, we have derived a CH inequality for electrons in a mesoscopic system in terms of the FCS formulated within the scattering approach. As a test of the CH inequality, we have applied it to an idealized system composed of an entangler, which produces Bell states, and conducting wires, that carry electrons into two spatially separated detectors. We have proved that the CH inequality is violated and we have analysed its behaviour in detail. We have then investigated the effect of dephasing occurring in the wires on the violation of the CH inequality and hence on the robustness of entanglement. To do so, we have implemented the fictitious reservoir model of Büttiker [48] and discussed its consequences. Finally, we have applied the CH inequality to a realistic mesoscopic structure consisting of a three-arm beam-splitter, proving that violation occurs in this system even though no interaction is present.

Acknowledgments

This work was supported by the FPI program of the Comunidad Autónoma de Madrid and the EU under the Marie Curie Research Training Network (EP); the grant NSF DMR-0210575 (LF); and by the EC through grants EC-RTN Nano, EC-RTN Spintronics and EC-IST-SQUIBIT2 (FT and RF).

References

- [1] Bell J S 1987 *Speakable and Unspeakable in Quantum Mechanics* (Cambridge: Cambridge University Press)
- [2] Nielsen M A and Chuang I L 2000 *Quantum Computation and Quantum Information* (Cambridge: Cambridge University Press)
- [3] Zeilinger A 1999 *Rev. Mod. Phys.* **71** S288
- [4] Rauschenbeutel A, Nogues G, Osnaghi S, Bertet P, Brune M, Raimond J-M and Haroche S 2000 *Science* **288** 2024
- [5] Sackett C A *et al* 2000 *Nature* **404** 256
- [6] Loss D and DiVincenzo D P 1998 *Phys. Rev. A* **57** 120
- [7] Makhlin Yu, Schön G and Shnirman A 2001 *Rev. Mod. Phys.* **73** 357
- [8] Awschalom D D, Loss D and Samarth N (ed) 2002 *Semiconductor Spintronics and Quantum Computation (Series on Nanoscience and Technology)* (Berlin: Springer)
- [9] Recher P, Sukhorukov E V and Loss D 2001 *Phys. Rev. B* **63** 165314
- [10] Lesovik G B, Martin T and Blatter G 2001 *Eur. J. Phys. B* **24** 287
- [11] Samuelsson P, Sukhorukov E V and Büttiker M B 2003 *Phys. Rev. Lett.* **91** 157002
- [12] Recher P and Loss D 2003 *Phys. Rev. Lett.* **91** 267003
- [13] Prada E and Sols F 2004 *Eur. J. Phys. B* **40** 379
- [14] Samuelsson P, Sukhorukov E V and Büttiker M B 2004 *Phys. Rev. B* **70** 115330
- [15] Sauret O, Feinberg D and Martin T 2004 *Preprint cond-mat/0402416*
- [16] Recher P and Loss D 2002 *Phys. Rev. B* **65** 165327
- [17] Bena C, Vishveshwara S, Balents L and Fisher M P A 2002 *Phys. Rev. Lett.* **89** 037901
- [18] Bouchiat V, Chtchelkatchev N, Feinberg D, Lesovik G B, Martin T and Torres J 2003 *Nanotechnology* **14** 77
- [19] Oliver W D, Yamaguchi F and Yamamoto Y 2002 *Phys. Rev. Lett.* **88** 037901
- [20] Saraga D S and Loss D 2003 *Phys. Rev. Lett.* **90** 166803
- [21] Beenakker C W J, Kindermann M, Marcus C M and Yacoby A 2004 *Fundamental Problems of Mesoscopic Physics* ed I V Lerner, B L Altshuler and Y Gefen (*NATO Science Series II* vol 154) (Dordrecht: Kluwer)
- [22] Costa A T and Bose S 2001 *Phys. Rev. Lett.* **87** 277901
- [23] Beenakker C W J, Emary C, Kindermann M and van Velsen J L 2003 *Phys. Rev. Lett.* **91** 147901

- [24] Lebedev A V, Lesovik G B and Blatter G 2005 *Phys. Rev. B* **71** 045306
- [25] Lebedev A V, Blatter G, Beenakker C W J and Lesovik G B 2005 *Phys. Rev. B* **69** 235312
- [26] Lebedev A V, Lesovik G B and Blatter G 2005 *Preprint* cond-mat/0504583
- [27] Samuelsson P, Sukhorukov E V and Büttiker M 2004 *Phys. Rev. Lett.* **92** 026805
- [28] Beenakker C W J and Kindermann M 2004 *Phys. Rev. Lett.* **92** 056801
- [29] Beenakker C W J, Emary C and Kindermann M 2004 *Phys. Rev. B* **69** 115320
- [30] Samuelsson P and Büttiker M B 2004 *Preprint* cond-mat/0410581
- [31] Saraga D S, Altshuler B L, Loss D and Westervelt R M 2004 *Preprint* cond-mat/0408362
- [32] Burkard G, Sukhorukov E V and Loss D 2000 *Phys. Rev. B* **61** 16303
- [33] Taddei F and Fazio R 2002 *Phys. Rev. B* **65** 075317
- [34] Bell J S 1964 *Physics* **1** 195
- [35] Wootters W K 1998 *Phys. Rev. Lett.* **80** 2245
- [36] Kawabata S 2001 *J. Phys. Soc. Japan* **70** 1210
- [37] Faoro L, Taddei F and Fazio R 2004 *Phys. Rev. B* **69** 125326
- [38] Samuelsson P, Sukhorukov E V and Büttiker M 2003 *Turk. J. Phys.* **27** 481
- [39] van Velsen J L, Kindermann M and Beenakker C W J 2003 *Turk. J. Phys.* **27** 323
- [40] Burkard G and Loss D 2003 *Phys. Rev. Lett.* **91** 087903
- [41] Clauser J F and Horne M A 1974 *Phys. Rev. D* **10** 526
- [42] Mandel L and Wolf E 1995 *Optical Coherence and Quantum Optics* (Cambridge: Cambridge University Press)
- [43] Nazarov Yu V 1999 *Ann. Phys. (Lpz.)* **8** (Spec. Issue) SI-193
- [44] Belzig W and Nazarov, Yu V 2001 *Phys. Rev. Lett.* **87** 067006
Belzig W and Nazarov Yu V 2001 *Phys. Rev. Lett.* **87** 197006
- [45] Levitov L S 2003 *Quantum Noise in Mesoscopic Physics* ed Yu V Nazarov (Amsterdam: Kluwer)
Kindermann M and Nazarov Yu V 2003 *Quantum Noise in Mesoscopic Physics* ed Yu V Nazarov (Amsterdam: Kluwer)
Bagrets D A and Nazarov Yu V 2003 *Quantum Noise in Mesoscopic Physics* ed Yu V Nazarov (Amsterdam: Kluwer)
Belzig W 2003 *Quantum Noise in Mesoscopic Physics* ed Yu V Nazarov (Amsterdam: Kluwer)
- [46] Büttiker M 1992 *Phys. Rev. B* **46** 12485
- [47] Prada E, Taddei F and Fazio R 2005 *Preprint* cond-mat/0505579
- [48] Büttiker M 1986 *Phys. Rev. B* **33** 3020
- [49] Büttiker M 1988 *IBM J. Res. Dev.* **32** 63
- [50] Landauer R 1957 *IBM J. Res. Dev.* **1** 223
Büttiker M 1986 *Phys. Rev. Lett.* **57** 1761
Szafer A and Stone A D 1988 *IBM J. Res. Dev.* **32** 384
- [51] Beenakker C W J and Büttiker M 1992 *Phys. Rev. B* **46** 1889
- [52] Blanter Ya M and Büttiker M 2000 *Phys. Rep.* **336** 1
- [53] Seelig G and Büttiker M 2001 *Phys. Rev. B* **64** 245313
- [54] Marquardt F and Bruder C 2004 *Phys. Rev. B* **70** 125305
- [55] Pala M G and Iannaccone G 2004 *Phys. Rev. B* **69** 235304
- [56] Pala M G and Iannaccone G 2004 *Phys. Rev. Lett.* **93** 256803
- [57] Förster H, Pilgram S and Büttiker M 2005 *Preprint* cond-mat/0502400
- [58] Büttiker M, Imry Y and Azbel M Ya 1984 *Phys. Rev. A* **30** 1982
- [59] Datta S 1995 *Electronic Transport in Mesoscopic Systems* (Cambridge: Cambridge University Press)
- [60] Brataas A, Nazarov Yu V and Bauer G E W 2001 *Eur. J. Phys. B* **22** 99
- [61] Muzykantskii B A and Khmel'nitskii D E 1994 *Phys. Rev. B* **50** 3982
- [62] Levitov L S and Lesovik G B 1993 *Pis'ma Zh. Eksp. Teor. Fiz.* **58** 225
Levitov L S and Lesovik G B 1993 *JETP Lett.* **58** 225 (Engl. Transl.)
- [63] Levitov L S, Lee H and Lesovik G B 1996 *J. Math. Phys.* **37** 10
- [64] Bose S and Home D 2002 *Phys. Rev. Lett.* **88** 050401